of destabilizing $C_1(\pi)$–$C_4(\pi)$ interactions in the former compounds. The value of AE_1 and AE_2 in thiophene (**6**) is consistent with stabilizing interactions between the C_1 and C_4 $p(\pi)$ orbitals and the d_{yz} and d_{xy} orbitals on sulfur in π_3* and π_4*, respectively.

Acknowledgment. We thank the National Science Foundation for support of this work (Grants CHE77-14930 and CHE78-12218) and the Gillette Research Foundation for a fellowship to J.C.G.

Electronic Spectroscopy of a Diplatinum(II) Octaphosphite Complex

W. A. Fordyce, J. G. Brummer, and G. A. Crosby*

Contribution from the Department of Chemistry and the Chemical Physics Program, Washington State University, Pullman, Washington 99164. *Received April 20, 1981*

Abstract: Fluorescence and phosphorescence have been observed at room temperature and at 77 K from a P–O–P bridged Pt(II) dimer. The terms assigned to these emissions, $^1A_{2u}$ and $^3A_{2u}$, respectively, were also observed in the absorption and excitation spectra. The low-temperature (~77 K) phosphorescence spectrum of the solid exhibited vibrational fine structure, which we have subjected to a Franck–Condon analysis. The prominent 118-cm^{-1} progression corresponds to the symmetrical stretching vibration of the Pt centers. We conclude that the electronic transition is $\sigma^*(5d_z) \rightarrow \sigma(6p_z)$. Low-temperature results indicate a weak spin–orbit splitting of the $^3A_{2u}$ term into E_u (τ = 1.58 μs) and A_{1u} (τ = 880 μs) components separated by 49.6 cm^{-1}.

In 1977 Sperline et al.[1] reported the preparation of a Pt complex isolated from a K_2PtCl_4–H_3PO_3 melt that exhibited an intense luminescence in aqueous solution. Subsequently Sadler et al.[2] characterized the complex by X-ray crystallography as an octaphosphite Pt(II) dimer bridged by four $(HO)OP–O–PO(OH)^{2-}$ linkages in an eclipsed configuration with a Pt–Pt distance of 2.925 Å.

Our interest in this species was sparked by the similarity of the face-to-face square planes of the dimer with the columnar structure of $[Pt(CN)_4]^{2-}$ complexes in the solid state[3] and the existence of intense luminescence from both systems. These similarities suggested to us that the dimer may model the Pt–Pt interactions in solids containing the $[Pt(CN)_4]^{2-}$ ion. In addition the Pt(II) dimer complex is isostructural and isoelectronic in the d shell with $[Rh_2(bridge)_4]^{2+}$ (bridge = 1,3-diisocyanopropane), a substance that has been extensively studied by Gray and co-workers.[4] Thus, we hoped that a study of the electronic character of the Pt(II) complex would also provide insight into the electronic structure of the Rh(I) complex and those of the less extensively investigated diphosphine-bridged isocyanide Rh(I) dimers.[5]

We report here the observation of both a fluorescence and a phosphorescence from the Pt dimer $[Pt_2(pop)_4]^{4-}$. The terms responsible for these emissions have also been observed in the absorption and excitation spectra. Moreover, the low-temperature (<77 K) phosphorescence spectrum of the solid exhibits a pronounced vibrational fine structure that has yielded geometrical information via a Franck–Condon analysis (FCA). Finally the spin–orbit splitting of the manifold responsible for the phosphorescence has been determined from the results of low-temperature lifetime measurements and related to the orbital character of the term.

Experimental Section

The complex $K_4[Pt_2H_8P_8O_{20}]\cdot 2H_2O$ ($[Pt_2(pop)_4]^{4-}$) was prepared as dark green crystals by the method of Sadler et al.[2] All computations and spectral data acquisition were accomplished with a Digital 11/34 system. Spectra were plotted with a Tektronix 4662 digital plotter. Absorption spectra were recorded on a Cary 14 spectrophotometer, and room temperature emission and excitation spectra were obtained on a Hitachi MPF-2A spectrofluorimeter. At 77 K in a Nujol mull the phosphorescence excitation spectrum of $[Pt_2(pop)_4]^{4-}$ was measured by exciting the sample with the output from a 1000-W tungsten–iodide lamp passed through a Spex Doublemate monochromator (0.5-nm resolution). The variation in phosphorescence intensity was monitored by a detection system consisting of a Spex Minimate monochromator and a thermoelectrically cooled RCA C31034A photomultiplier.

For the Franck–Condon studies low-temperature phosphorescence spectra were obtained by exciting solid samples with light from a 150-W Hg lamp filtered through 5 cm of an aqueous $CuSO_4$ solution (100 g/L) and a Corning 7-60 glass filter. Scattered exciting light was blocked by a Corning 3-73 glass cut-off filter located before the entrance slit of a 0.5-m Jarrell-Ash monochromator. Resolution was sample limited. The signal from a thermoelectrically cooled RCA C31034A photomultiplier was amplified with a Keithley picoammeter. The sample temperature was controlled in an Andonian Model 0-24/7 M-H dewar described previously.[6] All emission spectra were corrected for monochromator and photomultiplier efficiency. Excitation spectra were also corrected for monochromator efficiency and variations of lamp intensity.

Lifetimes of the phosphorescence were obtained as a function of temperature by exciting the sample in a 2:1 ethylene glycol/water glass with a Molectron UV-22 nitrogen laser. The emitted light was filtered through a KNO_2 solution, detected with an EMI 9558B photomultiplier wired for fast response,[7] and displayed on a Tektronix 549 oscilloscope. Lifetimes were determined by a linear least-squares fit of ln intensity vs. time. The sample temperature was controlled as indicated above.

Results

Absorption, Emission, and Excitation Spectra. The absorption spectrum of $[Pt_2(pop)_4]^{4-}$ in water at room temperature is shown in Figure 1. The spectrum is characterized by four maxima at 22 100 cm^{-1} (ϵ = 120 M^{-1} cm^{-1}), 27 200 cm^{-1} (33 500), 33 000 cm^{-1} (849), and 37 000 cm^{-1} (1360). The extinction coefficient and position of the maximum at 27 200 cm^{-1} is in general agreement with the spectrum reported by Sadler et al.[2] The positions of the two highest energy maxima agree with those previously reported, but the extinction coefficients we report are substantially lower; the discrepancy may be due to the fact that we recorded the absorption spectrum of a crystallized sample. The relatively weak lowest energy absorption maximum has not been

(1) Sperline, R. P.; Dickson, M. K.; Roundhill, D. M. *J. Chem. Soc., Chem. Commun.* **1977**, 62.
(2) Filomena Dos Remedios Pinto, M. A.; Sadler, P. J.; Neidle, S.; Sanderson, M. R.; Subbiah, A. *J. Chem. Soc., Chem. Commun.* **1980**, 13.
(3) Yersin, H.; Gliemann, G. *Ann. N.Y. Acad. Sci.* **1978**, *313*, 539 and references therein.
(4) Mann, K. R.; Thich, J. A.; Bell, R. A.; Coyle, C. L.; Gray, H. B. *Inorg. Chem.* **1980**, *19*, 2462 and references therein.
(5) Balch, A. L.; Tulyathan, B. *Inorg. Chem.* **1977**, *16*, 2840.
(6) Harrigan, R. W.; Crosby, G. A. *J. Chem. Phys.* **1973**, *59*, 3468.
(7) Demas, J. N.; Flynn, C. M. *Anal. Chem.* **1976**, *48*, 353.

0002-7863/81/1503-7061$01.25/0

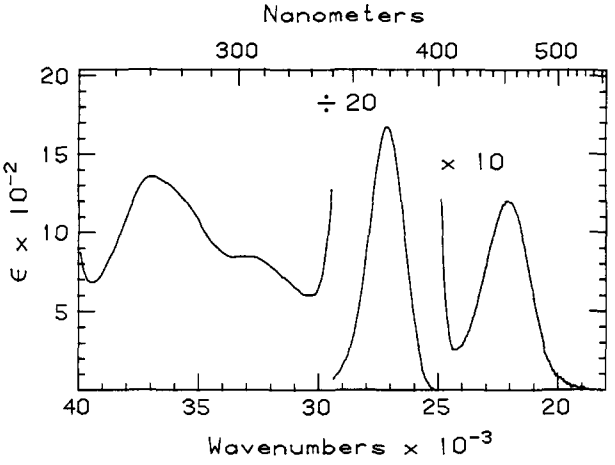

Figure 1. Room-temperature absorption spectrum of $[Pt_2(pop)_4]^{4-}$ in water.

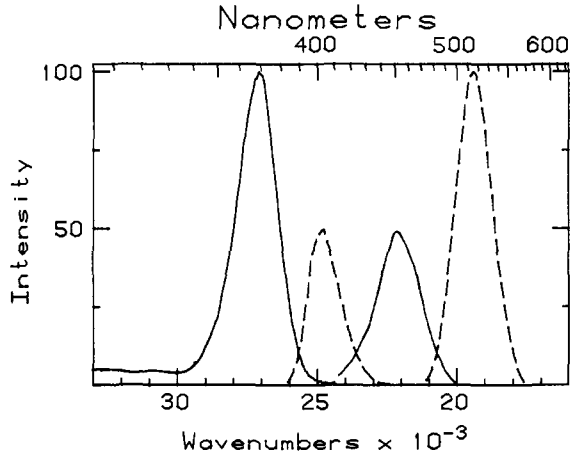

Figure 2. Room-temperature emission (----) and excitation (—) spectra of $[Pt_2(pop)_4]^{4-}$ in water. Relative peak heights are arbitrary.

previously reported. In a Nujol mull the absorption spectrum of the solid recorded at temperatures between 77 and 13 K[8] reveals maxima at 21 400, 25 200, 33 400, and 36 800 cm^{-1}.

The emission and excitation spectra of $[Pt_2(pop)_4]^{4-}$ in water at room temperature are shown in Figure 2. Two emissions are observed, an intense green band (phosphorescence) at 19 400 cm^{-1} and a much weaker band (fluorescence) at 24 800 cm^{-1}. The phosphorescence excitation spectrum reveals transitions maximizing at 22 000 and 27 100 cm^{-1} that overlap the phosphorescence and fluorescence bands, respectively. The fluorescence excitation spectrum maximizes at 27 100 cm^{-1} and overlaps the emission. Except for small energy shifts the emission and excitation spectra of $[Pt_2(pop)_4]^{4-}$ in 2:1 ethylene glycol/water at 77 K are identical with those described above.

The phosphorescence spectrum of a solid sample of $[Pt_2(pop)_4]^{4-}$ at 75.4 K and the uncorrected excitation spectrum of a Nujol mull at 77 K are shown in Figure 3. Correction of the excitation spectrum did not significantly change the bandshape but only increased the noise on the band. Both spectra exhibit a prominent single vibrational progression. The spacings between vibrational peaks are 139 cm^{-1} (σ = 24) and 111 cm^{-1} (σ = 18) in the excitation and phosphorescence spectra, respectively. The spectra overlap at 20 330 cm^{-1}.

Low-Temperature Emission Spectra. The vibrational progression observed in the phosphorescence spectrum of a solid sample of $[Pt_2(pop)_4]^{4-}$ (see Figure 3) sharpens considerably as the temperature is lowered. Below 10 K the band begins to lose definition, and the maximum shifts from 19 400 (10 K) to 19 100

(8) Sample temperature was controlled with an Air Products Displex Model CSW-202.

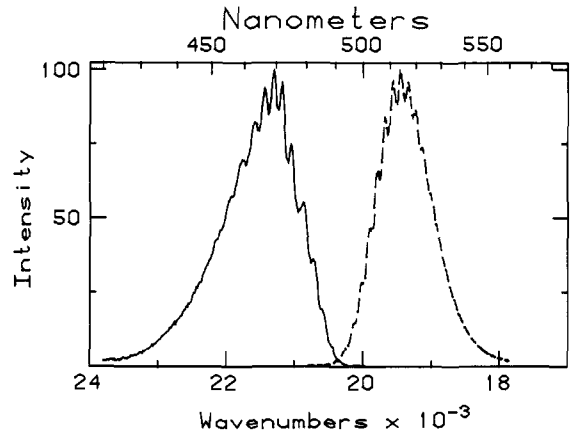

Figure 3. Phosphorescence excitation (—, 77 K, Nujol mull) and phosphorescence (----, 75.4 K, solid) spectra of $[Pt_2(pop)_4]^{4-}$.

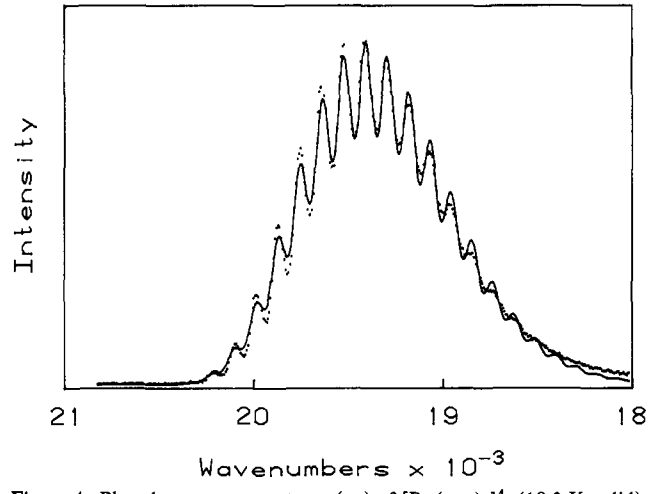

Figure 4. Phosphorescence spectrum (···) of $[Pt_2(pop)_4]^{4-}$ (10.3 K, solid) and computer-generated "best fit" Franck–Condon envelope (—).

cm^{-1} (1.71 K). The spectrum at 10.3 K is shown in Figure 4. We have subjected the band envelope to a Franck–Condon analysis, the theoretical basis of which has been described previously.[9] For convenience the definitions of the fitting parameters are given here. The ground-state vibrational frequency and anharmonicity are denoted by ω_0 and χ, respectively; the ratio of the excited-state to the ground-state vibrational frequency is $k^2 \equiv \omega'/\omega_0$; the normalized displacement coordinate is $b \equiv \Delta Q(M\omega_0/h)^{1/2}$; the apparent origin of the transition is denoted by α, which is red shifted from the 0–0 transition by the energy of any allowing mode(s). The set of fitting parameters is completed with w (full width at $1/e$ height of a single vibrational peak) and an arbitrary scaling factor.

The procedure for obtaining best fit values to the data set (800 points; every other point has been omitted in Figure 4 for clarity) through optimizing by discrete variation of α is described by Mazur and Hipps.[10] The results are as follows: α = 20 330 cm^{-1}, χ = 0.26 cm^{-1}, ω_0 = 118 cm^{-1}, k^2 = 0.72, and b = 4.57.

Emission Lifetimes. The measured phosphorescence lifetime in a deoxygenated aqueous solution at room temperature is 5.5 μs (5.7 μs in deoxygenated 2:1 ethylene glycol/water). At 77 K in 2:1 ethylene glycol/water the phosphorescence lifetime of $[Pt_2(pop)_4]^{4-}$ is 10.3 μs. This small increase in the measured phosphorescence lifetime upon cooling indicates a large room-temperature phosphorescence quantum yield (~50%), an unusually high value. As the temperature is lowered below 77 K,

(9) (a) Hipps, K. W.; Merrell, G. A.; Crosby, G. A. *J. Phys. Chem.* **1976**, *80*, 2232. (b) Hipps, K. W.; Merrell, G. A.; Crosby, G. A. *Ibid.* **1978**, *82*, 1454; (c) Merrell, G. A. Ph.D. Dissertation, Washington State University, Pullman, WA, 1979.

(10) Mazur, U.; Hipps, K. W. *J. Phys. Chem.* **1980**, *84*, 194.

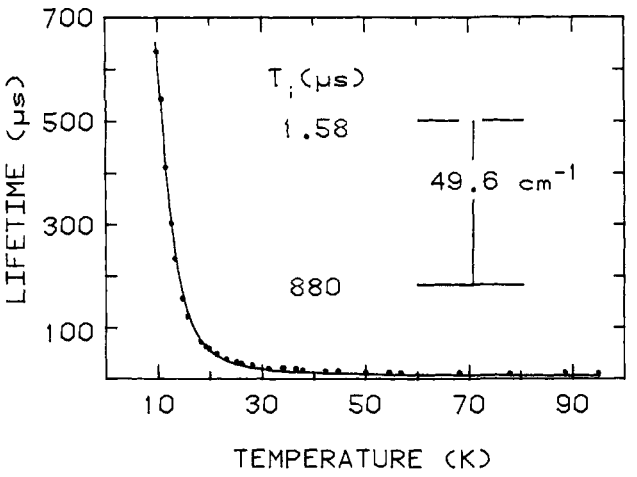

Figure 5. Temperature dependence of the lifetime of $[Pt_2(pop)_4]^{4-}$ in 2:1 ethylene glycol/water (···) and computer-generated "best fit" curve (—) with resultant energy level scheme.

however, the lifetime increases dramatically (Figure 5). At temperatures between 95 and 9 K the decay is exponential over a period of at least two lifetimes, but below 9 K the decay becomes nonexponential.

Our method of analysis of the lifetime results between 95 and 9 K, which is based on two emitting levels in Boltzmann equilibrium, is identical with that described previously.[11] The computer-generated fit and resultant level scheme is shown in Figure 5. The degeneracy factor of 2 for the higher level in the emitting manifold is not derivable from the experimental data but is consistent with the proposed term assignments (vide infra).

Discussion

The similarity in the major features of the absorption spectrum of $[Pt_2(pop)_4]^{4-}$ obtained in water and in a Nujol mull and the observation of the phosphorescence in both media indicate that the dimeric structure confirmed for the solid state is preserved in solution. Coincidence of the peaks in the emission excitation spectra with the two lower energy peaks in the absorption spectrum verifies that both emissions originate from $[Pt_2(pop)_4]^{4-}$. The orbitals (D_{4h} symmetry) and their ordering pertinent to the electronic description of the complex are assumed to be $1a_{1g}$ ($5d_{z^2}$) < $1a_{2u}$ ($5d_{z^2}$) < $2a_{1g}$ ($6p_z$) < $2a_{2u}$ ($6p_z$).[12] The $1a_{1g}$ and $1a_{2u}$ orbitals are both occupied in the ground state; consequently the lowest energy allowed transition is $^1A_{1g} \rightarrow {}^1A_{2u}$ ($^1a_{2u} \rightarrow 2a_{1g}$). We assign the absorption peak in water at 27 200 cm^{-1} (25 200 cm^{-1} in a Nujol mull) to this transition and the weak emission at 24 800 cm^{-1} to the corresponding fluorescence. The weak absorption peak in water at 22 100 cm^{-1} (21 400 in a Nujol mull) is assigned to the $^1A_{1g} \rightarrow {}^3A_{2u}$ ($1a_{2u} \rightarrow 2a_{1g}$) transition and the intense emission at 19 400 cm^{-1} (19 500 cm^{-1} in a Nujol mull) to the corresponding phosphorescence.

Recently Ellenson et al.[13] have observed both fluorescence and phosphorescence from single crystals of $BaPd(CN)_4 \cdot 4H_2O$ upon nitrogen laser excitation. It is probable that other columnar structures exhibit two emissions also, but unless excited with intense pulsed sources, any weak fluorescence could remain undetected.

The exceptionally weak $^1A_{1g} \rightarrow {}^3A_{2u}$ absorption is in contrast to that observed in Rh(I) and Ir(I) monomeric complexes. For the complexes $[M(2{=}phos)_2]^+$ [M = Rh(I) and Ir(I)] $\epsilon(^1A_{1g} \rightarrow {}^1A_{2u})/\epsilon(^1A_{1g} \rightarrow {}^3A_{2u})$ is approximately 26 and 6, respectively.[14] For $[Pt_2(pop)_4]^{4-}$ the ratio is 270. Miskowski et al.[15] have suggested for $[Rh_2(bridge)_4]^{2+}$ that spin–orbit mixing of the $E_u(^3A_{2u})$ term with $E_u(^1E_u)$ terms is considerably less in dimeric complexes than in the monomeric species because of the large energy gaps between the terms. This larger gap between intensity borrowing terms and the inherently weak spin–orbit coupling in $[Pt_2(pop)_4]^{4-}$ (vide infra) lead to an unexpectedly weak $^1A_{1g} \rightarrow {}^3A_{2u}$ transition.

Franck–Condon Analysis. The value of α (20 330 cm^{-1}) obtained from the FCA is in excellent agreement with the energy of the overlap region of the excitation and emission spectra shown in Figure 3 and indicates that the phosphorescence at 10.3 K is formally allowed. The small anharmonicity, χ, points to a deep potential well for the ground state. The ground-state vibrational frequency of 118 cm^{-1} derived from the FCA is indicative of a Pt–Pt stretching vibration and agrees with the Raman data from a solid sample of $[Pt_2(pop)_4]^{4-}$, which has a peak at 115 cm^{-1}. The latter is absent in the Raman spectrum of the related monomeric complex $Pt[P(OH)(OMe)_2]_2[P(O)(Me)_2]_2$. Pt–P stretching vibrations are ruled out for the progression, since they fall within the 300–450 cm^{-1} range for complexes with a square-planar geometry.[16,17]

Numerous authors[12,18,19] have described the lowest unoccupied orbital of Rh(I) dimers as possessing mixed p_z and π^*_{ligand} character. Similar descriptions have been made for the orbitals of $[Pt(CN)_4]^{2-}$ complexes in the solid state.[3] On the basis of the unique progression of the Pt–Pt stretching mode superimposed on the $[Pt_2(pop)_4]^{4-}$ bands, we see no need to include π^*_{ligand} character in the lowest unoccupied orbital and consequently assign the lowest-energy transition to $\sigma^*(5d_{z^2}) \rightarrow \sigma(6p_z)$.[20]

The value of k^2 equal to 0.72 from the FCA indicates an excited state vibrational frequency that is less than that of the ground state. The proposed orbital ordering for $[Pt_2(pop)_4]^{4-}$ (vide supra) predicts a formal Pt–Pt bond order of zero in the ground state. One can obtain weak Pt–Pt bonding, however, in the ground state by mixing the a_{1g} and a_{2u} orbital states, respectively.[14] In the lowest excited state a formal bond order of 1.0 exists. Thus one would expect a contraction of the Pt–Pt distance upon excitation and an increase in the frequency of the Pt–Pt stretching vibration contrary to our FCA result.

Theoretical work[9c] has shown that the FCA fitting procedure is not particularly sensitive to the value of k^2. In addition, Mazur and Hipps[10] have proposed that k^2 of solids is controlled not only by the force constant between the vibrating moieties but also by the crystalline environment. The values of the vibrational frequencies in the excited and ground states obtained directly from the phosphorescence excitation and phosphorescence spectra, shown in Figure 3, give a k^2 value of 1.25, but it should be noted that considerable scatter exists in these data. From the results presented here we are unable to determine definitively whether the complex expands or contracts upon excitation. On the basis of the proposed orbital model, however, we opt for a contraction.

For a symmetric distortion along the Pt–Pt axis, $\Delta r = b(2M\omega_0/h)^{-1/2}$ where M is the reduced mass of the Pt centers. If the vibration involves the entire Pt planes, Δr = 0.279 Å is obtained. If the vibration is a motion of the Pt atoms only, Δr = 0.438 Å. These displacements yield a 9.5% or 15% change in the Pt–Pt distance, respectively.

Emission Lifetimes. The phosphorescence lifetime vs. temperature results for $[Pt_2(pop)_4]^{4-}$, τ_{higher} = 1.58 μs and τ_{lower} = 880 μs, indicate that emission from the higher level is a partially allowed transition, whereas emission from the lower level is forbidden.[21] Formally, the $^3A_{2u}$ term will split under spin–orbit

(11) Fordyce, W. A.; Rau, H.; Stone, M. L.; Crosby, G. A. *Chem. Phys. Lett.* **1981**, *77*, 405.
(12) Mann, K. R.; Gordon, J. G., II; Gray, H. B. *J. Am. Chem. Soc.* **1975** *97*, 3553.
(13) Ellenson, W. D.; Viswanath, A. K.; Patterson, H. H. *Inorg. Chem.* **1981**, *20*, 780.
(14) Geoffroy, G. L.; Wrighton, M. S.; Hammond, G. S.; Gray, H. B. *J. Am. Chem. Soc.* **1974**, *96*, 3105.
(15) Miskowski, V. M.; Nobinger, G. L.; Klinger, D. S.; Hammond, G. S.; Lewis, N. S.; Mann, K. R.; Gray, H. B. *J. Am. Chem. Soc.* **1978**, *100*, 485.
(16) Adams, D. M.; Chandler, P. J. *J. Chem. Soc. A*, **1969**, 588.
(17) Neruda, B.; Lörberth, J. *J. Organomet. Chem.* **1976**, *111*, 241.
(18) Balch, A. L. *J. Am. Chem. Soc.* **1976**, *98*, 8049.
(19) Mague, J. T.; DeVries, S. H. *Inorg. Chem.* **1980**, *19*, 3743.
(20) Since the completion of this work Rice and Gray have reported reaching a similar conclusion for $[Rh_2(bridge)_4]^{2+}$. Rice, S. F.; Gray, H. B. *J. Am. Chem. Soc.* **1981**, *103*, 1593.
(21) The emission intensity decreased slightly as the temperature was lowered. We infer that the quantum yield of the lower level is less than that of the higher level.

coupling into E_u and A_{1u} components, which are dipole allowed (x, y) and forbidden, respectively. We therefore assign the shorter-lived higher-energy emitting level to the E_u allowed state in agreement with the FCA analysis, and the lower-energy emitting level to A_{1u}.

The free-ion spin-orbit coupling constant ξ_{5d} for Pt(II) is ~4000 cm^{-1}.[22] The ~50 cm^{-1} spin-orbit splitting of the $^3A_{2u}$ term obtained from the lifetime vs. temperature data seems quite small for a metal-centered term. We propose that the small splitting is due to exceptionally small orbital angular momentum in this $^3A_{2u}$ term. The weak spin-orbit coupling also manifests itself in the nonexponential lifetimes observed at temperatures below 9 K, reminescent of organic molecules.[23] In this view the relaxation rate between the levels in the $^3A_{2u}$ manifold below 9 K becomes comparable to or less than the radiative rates from the levels producing nonexponential decays and the observed spectral changes.

Application of the Strickler-Berg formula[24] to the strong absorption band leads to a predicted fluorescence radiative lifetime of 5.7 ns, well below our detection limit. Although the intensity formula was derived for strong singlet-singlet transitions, predictions for much weaker transitions will probably be correct within an order of magnitude.[24] If we assume that most of the intensity of the weak absorption band is carried by the $E_u(^3A_{2u})$ level, we calculate a phosphorescence radiative lifetime of 4.1 μs. If we make the reasonable assumption that the phosphorescence quantum yield is near unity at low temperature, then this calculated value is in good agreement with the measured lifetime from the $E_u(^3A_{2u})$ level of 1.58 μs.

Acknowledgment. This research was supported by the Air Force Office of Scientific Research (Grant AFOSR-80-0038) and the National Science Foundation (Grant DMR-78-10008). We are grateful to M. K. Dickson for bringing the intense luminescence of this complex to our attention and Professor K. W. Hipps for suggesting the low-temperature solid-state experiments. We would also like to thank Dr. J. J. Freeman (Monsanto Corp.) for obtaining the Raman spectra.

(22) Griffith, J. S. "The Theory of Transition Metal Ions"; Cambridge University Press: London, 1964; p 113.
(23) El-Sayed, M. A. *Acc. Chem. Res.* **1971**, *4*, 23.
(24) Strickler, S. J.; Berg, R. A. *J. Chem. Phys.* **1962**, *37*, 814.

Three-Dimensional Structure of the Superconductor $(TMTSF)_2AsF_6$ and the Spin-Charge Separation Hypothesis

F. Wudl

Contribution from the Bell Laboratories, Murray Hill, New Jersey 07974.
Received April 28, 1981. Revised Manuscript Received July 8, 1981

Abstract: The structure of the organic superconductor $(TMTSF)_2AsF_6$ is described in detail. It is shown that the salts $(TMTSF)_2X$ (X = PF_6 and AsF_6) are *pseudo-two-dimensional*. A structure-related hypothesis is presented in which spin-charge separation and charge localization can be used to explain why there are no charge density waves in $(TMTSF)_2X$.

In the decade between our discovery of the electrical conductivity of the first chalcogenafulvalene salt [tetrathiafulvalenium chloride (TTFCl)[1,2]] and the discovery of high-pressure superconductivity of another chalcogenafulvalenium salt [bis(tetramethyltetraselenafulvalene) hexafluorophosphate[3,4] ($(TMTSF)_2PF_6$)], several important concepts have evolved.[5] These concepts were initially biased by the historical importance of tetracyanoquinodimethane (TCNQ). For example, in the first organic metal (TTF·TCNQ), it was maintained for years that TTF was just a polarizable counterion to TCNQ.[5f] In fact, we know now that all *highly* conductive organic metals are formed from radical ions based on chalcogenafulvalenoids[6] *and not on* TCNQ and are single stack lattices in which the metallic conductivity is due only to long-range delocalization among donors.[5]

Table I. Intensity Measurements

instrument:	Enraf-Nonius CAD4 diffractometer
monochromator:	graphite crystal, incident beam
attenuator:	Zr foil, factor 20.7
take-off angle:	2.8°
detector aperture:	2.0-2.6 mm horizontal; 2.0 mm vertical
crystal-to-detector dist:	21 cm
scan type:	ω-2θ
scan rate:	2-20°/min (in ω)
scan width:	$(0.7 + 0.350 \tan\theta)°$
max 2θ:	58.0°
no. of reflctns measd:	3832 total, 3815 unique
correctns:	Lorentz-polarization; empirical absorption (from 0.85 to 1.00 on I); extinction (coefficient = 0.000 000 6)

Prior to the advent of $(TMTSF)_2X$ (X = BF_4, ClO_4, PF_6, AsF_6, SbF_6, NO_3),[3] the principal requirements to achieve metallic be-

(1) Wudl, F.; Smith, G. M.; Hufnagel, E. J. *J. Chem. Soc. D* **1970**, 1453.
(2) Wudl, F.; Wobschall, D.; Hufnagel, E. J. *J. Am. Chem. Soc.* **1972**, *94*, 670.
(3) Bechgaard, K.; Jacobsen, C. S.; Mortensen, K.; Pedersen, H. J.; Thorup, N. *Solid State Commun.* **1980**, *33*, 1119.
(4) (a) Jerome, D.; Mazaud, A.; Ribault, M.; Bechgaard, K. *J. Phys. Lett.* **1980**, *41*, L95. (b) Andres, K.; Wudl, F.; McWhan, D. B.; Thomas, G. A.; Nalewajek, D.; Stevens, A. L. *Phys. Rev. Lett.* **1980**, *45*, 1449.
(5) (a) Alcacer, L., Ed. "The Physics and Chemistry of Low Dimensional Solids"; D. Reidel Publishing Co.: Dordrecht, Holland 1980. (b) Hatfield, W. E., Ed. "Molecular Metals"; Plenum Press: New York, 1979. (c) Miller, J. S.; Epstein, A. J., Eds. *Ann. N.Y. Acad. Sci.*, **1978**, *313*, "Synthesis and Properties of Low Dimensional Materials". (d) Keller, H. J., Ed. "Chemistry and Physics of One Dimensional Metals"; Plenum Press: New York, 1977. (e) Torrance, J. B. *Acc. Chem. Res.* **1979**, *12*, 79. (f) Garito, A. F.; Heeger, A. J. *Ibid.* **1974**, *7*, 232. (g) Soos, S. G. *Annu. Rev. Phys. Chem.* **1974**, *25*, 121.
(6) Other sulfur and selenium, nonfulvenoid donors also give rise to single-chain organic metals; i.e., P. Delhaes in ref. 5a, above. Perylene forms highly conducting PF_6 and AsF_6 salts (Keller, H. J.; Nothe, D.; Pritzkow, H.; Wehe, D.; Werner, M.; Koch, P.; Schweizer, D. *Mol. Cryst. Liquid Cryst.* **1981**, *62*, 181).

0002-7863/81/1503-7064$01.25/0